Stem Cell Reports, Volume *3*

Supplemental Information

Fast and Efficient Neural Conversion of Human Hematopoietic Cells

Julio Castaño, Pablo Menendez, Cristina Bruzos-Cidon, Marco Straccia, Amaia Sousa, Lorea Zabaleta, Nerea Vazquez, Amaia Zubiarrain, Kai-Christian Sonntag, Luisa Ugedo, Xonia Carvajal-Vergara, Josep Maria Canals, Maria Torrecilla, Rosario Sanchez-Pernaute, and Alessandra Giorgetti

Figure S1

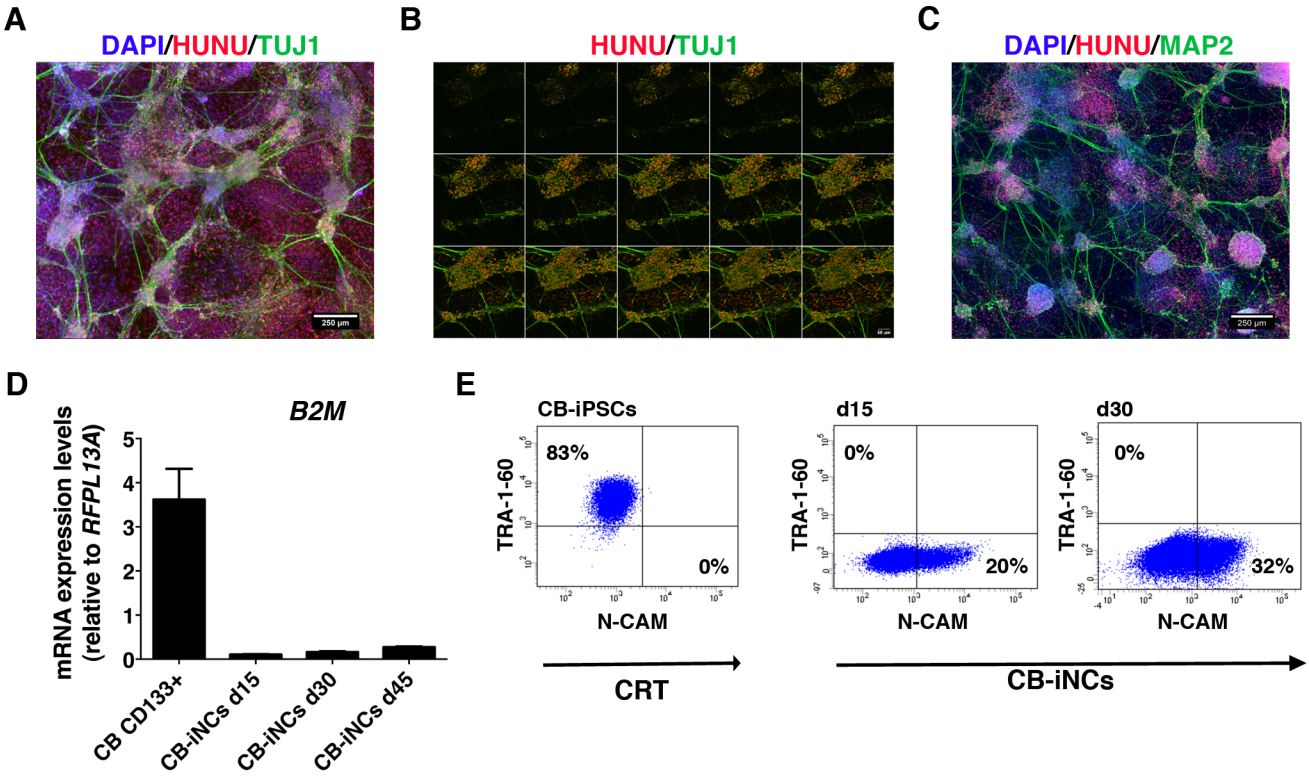
A
DAPI/HUNU/TUJ1
B
HUNU/TUJ1
C
DAPI/HUNU/MAP2
D
B2M
mRNA expression levels (relative to RFPL13A)
CB CD133+
CB-iNCs d15
CB-iNCs d30
CB-iNCs d45
E
CB-iPSCs
d15
d30
TRA-1-60
N-CAM
83%
0%
0%
20%
0%
32%
CRT
CB-iNCs

Figure S2

A

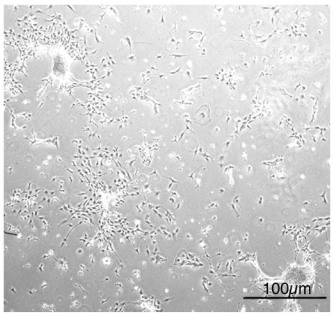

B

Figure S3

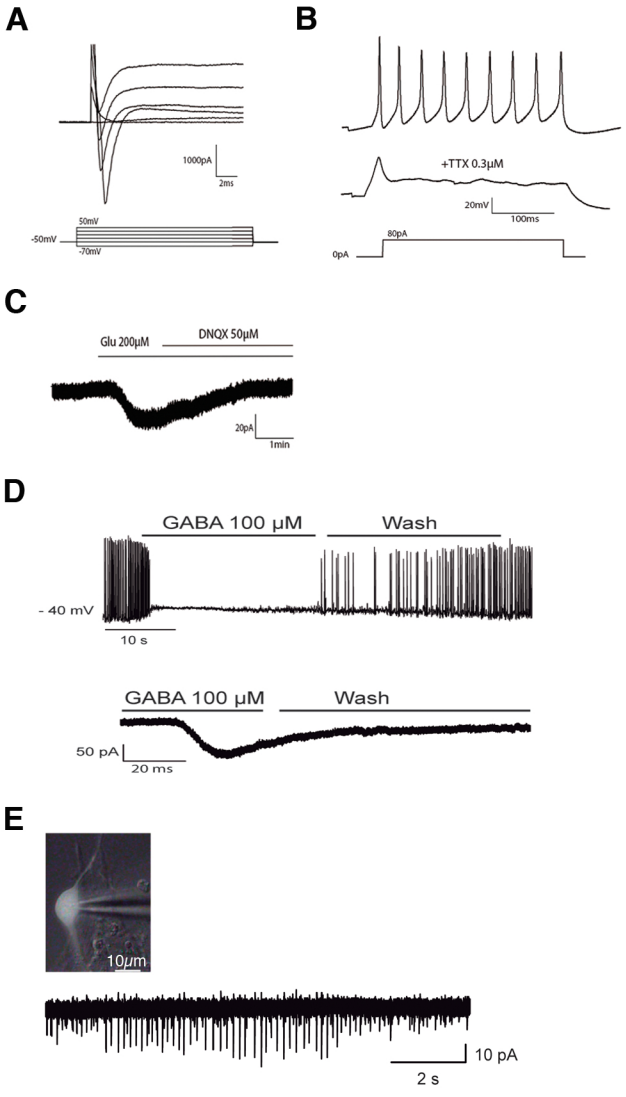
A
1000pA
2ms
50mV
-50mV
-70mV
B
+TTX 0.3µM
20mV
100ms
80pA
0pA
C
Glu 200µM
DNQX 50µM
20pA
1min
D
GABA 100 µM
Wash
- 40 mV
10 s
GABA 100 µM
Wash
50 pA
20 ms
E
10µm
10 pA
2 s

Figure S4

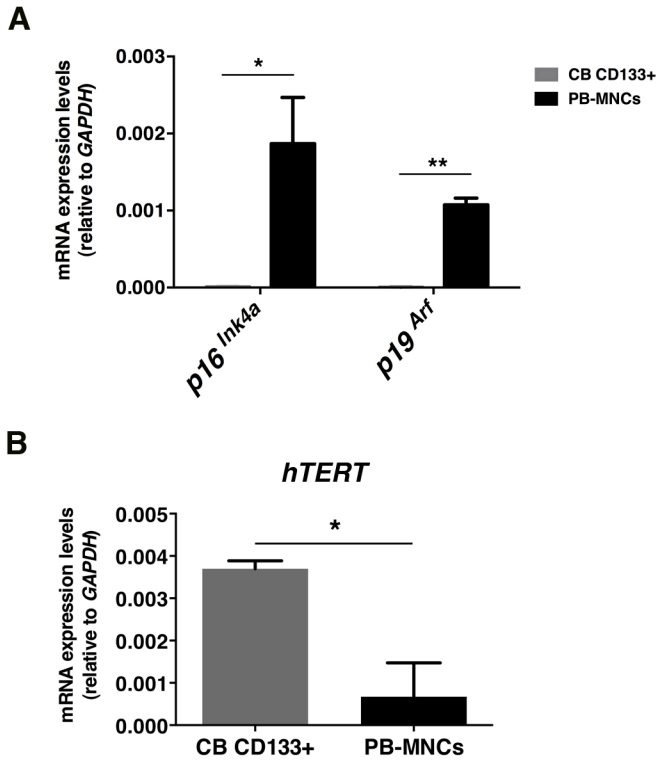
A
mRNA expression levels (relative to GAPDH)
0.003
0.002
0.001
0.000
*
**
CB CD133+
PB-MNCs
p16 Ink4a
p19 Arf
B
hTERT
mRNA expression levels (relative to GAPDH)
0.005
0.004
0.003
0.002
0.001
0.000
*
CB CD133+
PB-MNCs

Supplemental Figure Legends

Figure S1: CD133-positive CB cells induction into CB-iNCs

(A) Representative immunofluorescence tile image of overall culture morphology at day 30. CB-iNCs expressed the human nuclear antigen (HUNU) and were organized in TUJ1 positive clusters. Scale bar, as indicated in the panel.

(B) Z stack montage of representative CB-iNCs clusters; stacks were used to identify and quantify the number of HUNU/TUJ1 double positive cells at day 30 of neural induction**.** Scale bar, as indicated in the panel.

(C) Representative immunofluorescence tile image of CB-iNCs at day 30. CB-iNCs expressed the human nuclear antigen (HUNU) and were organized in clusters interconnected by fibres positive for MAP2. Scale bar, as indicated in the panel.

(D) qRT-PCR analysis showing the down-regulation of *B2M* in CB reprogrammed cells. Data are represented as mean ± SD (n=3 independent experiments).

(E) Flow cytometry analysis shows absence of TRA-1-60-positive cells within CB-iNCs at days 15 and 30 post-transduction. A CB-iPSC line was used as positive control for expression of TRA-1-60.

Figure S2: Chromosomal stability of thawed CB-iNCs

(A) Bright field microphotography of live cells after thawing (frozen at passage 7). Scale bar, as indicated in the panel.

(B) Representative high-resolution, G-banded karyotype showing a normal, diploid, female chromosomal content in CB-iNCs cells analysed after 60 passages.

Figure S3: Whole-cell patch-clamp recordings of CB-iNCs at day 65 of differentiation

(A) A representative trace of inward Na^+ and outward K^+ voltage-dependent currents triggered upon -70 mV to +50 mV voltage steps (V_h = -50 mV).

(B) Example of action potentials evoked by injecting a depolarizing current step (+80 pA) and the inhibitory effect of the Na+ channel blocker TTX (0.3 µM).

(C) A representative recording of a CB-iN cell from a different CB conversion experiment showing an inward current induced by glutamate and reversed by the non-NMDA receptor antagonist DNQX (V_h = -50 mV). Glutamate response was reliably obtained in all CB experiments, consistent with a high proportion of vGlut1-positive neurons in these conditions.

(D) Current-clamp recording from a CB-iN cell showing the inhibitory effect of GABA (100 µM) onto spontaneous action potentials (upper trace). Voltage-clamp recording of the inward current induced by GABA (V_h = -50 mV) (lower trace).

(E) A trace showing spontaneous activity recording from a SYN::GFP positive cell after thawing (V_h = -50 mV). Scale bar, as indicated in the panel.

Figure S4: Expression of *p16^{Ink4a}*, *p19^{Arf}* and *hTERT* in CD133-positive CB cells and PB-MNCs

(A) qRT-PCR analysis for mRNA levels of *p16^{Ink4a}* and *p19^{Arf}* at day 0 in fresh CD133-positive CB cells and PB-MNCs. Data are represented as mean ± SD (n=3 independent experiments). *p<0.05; **p<p0.001; unpaired, two-tailed t test.

(B) qRT-PCR analysis shows higher level of *hTERT* expression in CD133-positive CB cells when compared with PB-MNCs. Data are represented as mean ± SD (n=3 independent experiments). *p<0.05; unpaired, two-tailed t test.

Supplemental Tables

Table S1: Primary Antibodies used in this study

Antibody	Source	Dilution	Supplier
Doublecortin (DCX) (C-18)	Goat Polyclonal	1:500	sc- 8066 SCBT
GABA	Rabbit Polyclonal	1:500	A2052 Sigma
GFAP	Rabbit Polyclonal	1:500	Z0334 DakoCytomation
Human nuclei (HUNU)	Mouse Monoclonal	1:200	MAB1281, Millipore
Ki 67 (MIB1)	Mouse Monoclonal	1:500	DAKO
MAP2	Rabbit Polyclonal	1: 300	AB5622 Millipore
MAP2	Mouse Monoclonal	1:500	610460 BD Laboratories
NCAM (Eric 1)	Mouse Monoclonal	1:100	sc-106, SCBT
NESTIN	Mouse Monoclonal	1:250	MO15012 Neuromics
NEUN (FOX3)	Mouse Monoclonal	1:250	MAB337 Millipore
Neurofilament SMI 312	Mouse Monoclonal	1:500	NE1016 Calbiochem
PAX6	Mouse Monoclonal	1:200	DSHB Iowa University
PSD-95	Mouse Monoclonal	1:200	MA1-046 Thermo Fisher
SeV	Rabbit Polyclonal	1:500	MBL International Corporation
SNAP25	Rabbit Polyclonal	1:100	Ab41455 Abcam
SOX2	Goat Polyclonal	1:500	GT15098 Neuromics
SOX2	Goat polyclonal	1:300	AF2018 R&D
SV2	Mouse Monoclonal	1:50	DSH
Synapsin I	Mouse Monoclonal	1:100	Ab57467 Abcam
TAU (T46)	Mouse Monoclonal	1:500	136400, Invitrogen
vGLUT1	Guinea Pig Polyclonal	1:1000	AB5905, Chemicon International
vGLUT1	Rabbit Polyclonal	1:500	135003 Synaptic systems
β- III Tubulin (TUJ1)	Mouse Monoclonal	1:1000	mms-435p, Covance
β- III Tubulin (TUJ1)	Rabbit Polyclonal	1:500	ab6046, Abcam
β- III Tubulin (TUJ1)	Rabbit Polyclonal	1:1000	T2200 Sigma

Table S2: qRT-PCR primers used in this study

BRN2 Fw	5'-AATAAGGCAAAAGGAAAGCAACT-3'
BRN2 Rv	5'-CAAAACACATCATTACACCTGCT-3'
*MAP*2 Fw	5'-TAACCAACCACTGCCAGACCTGAA-3'
MAP2 Rv	5'-GCCACATTTGGATGTCACATGGCT-3′
PAX6 Fw	5′-CCGGCAGAAGATTGTAGAGC-3'
PAX6 Rv	5'-CGTTGGACACGTTTTGATTG-3′
NEUROD1 Fw	5'-AGCCCCAAGGTCCTCCAA-3'
NEUROD1 Rv	5'-CGTGCTCCTCGTCCTGAGA-3'
DCX Fw	5'-GCCAGGGAGAACAAGGACTTT-3'
DCX Rv	5'-CACCCCACTGCGGATGA-3'
NESTIN Fw	5'-GGGAAGAGGTGATGGAACCA-3'
NESTIN Rv	5'-AAGCCCTGAACCCTCTTTGC-3'
SOX1 Fw	5'-TCCCCCGCGTGAACTG-3'
SOX1 Rv	5'-CAAGGCATTTTGCGTTCACA-3'
SOX2 Fw	5'-CAAAAATGGCCATGCAGGTT-3'
SOX2 Rv	5'-AGTTGGGATCGAACAAAAGCTATT-3'
MASH1 Fw	5'-CTGGACTTTACCAACTGGTTCTGA-3'
MASH1 Rv	5'-CCTGCTTCCAAAGTCCATTCC-3'
NEUN Fw	5'-CCAAGCGGCTACACGTCT -3'
NEUN Rv	5'-GCTCGGTCAGCATCTGAG -3'
MUSASHI Fw	5'-GAGACTGACGCGCCCCAGCC-3'
MUSASHI Rv	5'-CGCCTGGTCCATGAAAGTGACG-3'

vGLUT Fw	5’-AGCCGCCGCATCATGT-3’
vGLUT Rv	5’-GCCTCCGCAGTTCATCAACT-3’
TUJ1 Fw	5’-AGTCGCCCACGTAGTTGC-3’
TUJ1 Rv	5’-CGCCCAGTATGAGGGAGAT-3’
TAU Fw	5’-CTCCAAAATCAGGGGATCGC-3’
TAU Rv	5’-CCTTGCTCAGGTCAACTGGT-3’
OCT4 Fw	5’-GGGTTTTTGGGATTAAGTTCTTCA-3’
OCT4 Rv	5’-GCCCCCACCCTTTGTGTT-3’
$p16^{Ink4}$ Fw	5’-GGGTCGGGTAGAGGAGGTG-3’
$p16^{Ink4}$ Rv	5’-ACCGTAACTATTCGGTGCGT-3’
$p19^{Arf}$ Fw	5’-TCTTGGTGACCCTCCGGATT-3’
$p19^{Arf}$ Rv	5’-CGGGATGTGAACCACGAAAAC-3’
TBR Fw	5’-CAACTCAGTCAACAGGAAGGC-3’
TBR Rv	5’-AAAGATGATCTCCAGCACAGC-3’
SeV Fw	5’-GGATCACTAGTGATATCGAGC-3’
SeV Rv	5’-ACCAGACAAGAGTTTAAGAGATATGTATC-3’
GAPDH Fw	5’-GCACCGTCAAGGCTGAGAAC-3’
GAPDH Rv	5’-AGGGATCTCGCTCCTGGAA-3’

Supplemental Experimental Procedures

RNA Purification and Quantitative RT-PCR

Isolation of total RNA from CD133-positive CB cells, CB-iNCs and PB-iNCs was performed using either RNeasy Mini Kit (Qiagen) or RNAqueous-Micro kit (Ambion) based on the cell number available. All RNA samples were treated with TURBO DNase (Ambion) to remove any residual genomic DNA and 1 ug of RNA was used to synthesize cDNA using the SuperScript III Reverse Transcriptase kit (Invitrogen). 25ng of cDNA were used to quantify gene expression by SybrGreen based Quantitative RT-PCR using the primers showed in Table S2 or by IDT primetime qPCR assay for the following genes *B2M* (Hs.PT.39a.22214845), *GAPDH* (Hs.PT.56a.40035104), *GATA4* (Hs.PT.42.776734), *HPRT1* (Hs.PT,51,2145446), *HSP90AB1* (Hs.PT.56a.38913643.gs), *RN18S1* (Hs.PT.39a.22214856.g), *RPL13A* (Hs.PT,51,21531404) and *BRACHYURY (T)* (Hs.PT.42.2366698). GraphPad Prism (v.5.01; GraphPad Software, Inc.) was used for statistical evaluation of the data. All statistical comparisons were made using Student *t* test. The level of significance was considered as $p \leq 0.05$.

Immunofluorescence (IF) analysis.

Cells cultured on coverslips were fixed with 4% paraformaldehyde in 1X PBS for 20 minutes at room temperature (RT). After rinsed with PBS cells were incubated in blocking buffer: 1X PBS with 10% normal donkey serum (Jackson Immunoresearch) and permeabilized with 0.1% Triton X-100 for 1 hour at RT. Coverslips were then incubated overnight at 4°C with primary antibodies in blocking buffer. After three washes in 1X PBS with 10% normal donkey serum the coverslips were incubated in Alexa Fluor-labelled secondary antibodies for 1 hour at RT and counterstained with Hoechst 33342 (Sigma-Aldrich) or DAPI before mounting using ProLong® antifade reagent (Molecular Probes®, Life Technologies). Stained cells were examined using an LSM510 Meta confocal microscope equipped with ultraviolet, argon, and helium-neon lasers

(Carl Zeiss, NY) and analyzed using Image J (1.42q http://rsb.info.nih.gov/ij). For identification of signal co-localization within a cell, optical thickness was kept to a minimum, and orthogonal reconstructions were obtained. On selected coverslips, the primary antibody was omitted to verify the specificity of the staining. Primary antibodies employed are listed in Table S1.

For quantification of the percentage of TUJ-1 and MAP2-positive cells, 50 images for Tuj1 and 192 images for MAP2 were taken randomly by a Leica AF6000 microscope with a 20x magnification objective. The area of each image was 640.8 x 478.88 μm. Manually *Count Objects* software from ImageJ was used to count the total number of HUNU positive nuclei and the TUJ1– and MAP2– double positive cells.

Karyotyping

Standard G-banding technique was performed at the Genetics Unit of Policlínica Gipuzkoa in random samples that were kept in culture for more than 20 passages (Catalina et al., 2008).

Suplemental References

Catalina, P., Montes, R., Ligero, G., Sanchez, L., de la Cueva, T., Bueno, C., Leone, P.E., and Menendez, P. (2008). Human ESCs predisposition to karyotypic instability: Is a matter of culture adaptation or differential vulnerability among hESC lines due to inherent properties? Mol Cancer 7, 76.